Inflammation, Vol. 42, No. 1, February 2019 (© 2018)
DOI: 10.1007/s10753-018-0876-6

ORIGINAL ARTICLE

A Novel Biological Role of α-Mangostin *via* TAK1–NF-κB Pathway against Inflammatory

Wenshu Zou,[1] Peng Yin,[2] Yaran Shi,[1] Na Jin,[1] Qian Gao,[1] Jiandong Li,[1] and Fenghua Liu[1,3]

Abstract— The oxysterone α-mangostin is isolated from mangosteen husks and is widely used in the treatment of abdominal pain, diarrhea, and dysentery. In this study, we established a lipopolysaccharide (LPS)-induced inflammatory model of rat intestinal epithelial cells (IEC-6 cells), at the same time we used differently concentration α-mangostin to detect its anti-inflammatory activity. We applied doses of α-mangostin (2.5, 5, and 10 μM) and detected apoptosis by flow cytometry, and the Griess reagent and the enzyme-linked immunosorbent assay (ELISA) method detected inflammatory factors such as nitric oxide (NO), prostaglandin (PG) E2, interleukin (IL)-1β, IL-6, and tumor necrosis factor (TNF)-α. We also used quantitative real-time PCR (Q-PCR) to examine inflammatory factors and western blotting to examine the activation of transforming growth factor-activated kinase (TAK)-1-nuclear factor (NF)-κB signaling pathway-related proteins. Finally, we used laser confocal microscopy to detect the effect of the 10 μM α-mangostin on the nuclear import of NF-κB–p65. The results showed that α-mangostin treatment significantly reduced the apoptosis of LPS-stimulated IEC-6 cells, the production of inflammatory factors, the activation of TAK1–NF-κB signaling pathway-related proteins, and the entry of p65 into the nucleus. In conclusion, α-mangostin exerts its anti-inflammatory effects by inhibiting the activation of TAK1–NF-κB and it may be a potential choice for the treatment of inflammation diseases.

KEY WORDS: α-mangostin; inflammatory; LPS; TAK1; NF-κB.

INTRODUCTION

As a complex organ, the intestine plays an important role in the growth and metabolism of the body. The intact intestinal mucosa acts as the first barrier to the intestinal tract, preventing physical, chemical, and biological factors from causing damage leading to inflammatory bowel disease, while the integrity of the intestinal mucosal epithelium depends mainly on the proliferation of monolayers of intestinal epithelial cells (IECs) [1, 2]. Inflammation is a complex set of interactions among soluble factors and cells that can arise in any tissue in response to traumatic, infectious, post-ischemic, or autoimmune injury [3]. LPS, as the main pathogenic component of Gram-negative bacteria, is often used as a stimulator of inflammation to regulate IL-6, TNF-α, and IL-1β secretion and activate the Toll-like receptor 4 (TLR4)/TLR2–MyD88–NF-κB signaling pathway [4, 5]; in addition, the model constructed by LPS stimulation often leads to an increase in the expression of pro-inflammatory cytokines NO and PGE2 [6, 7].

Mangosteen, the fruit of the evergreen tree mangosteen [8, 9], has been used as a traditional medicine for the treatment

[1] College of Animal Science and Technology, Beijing University of Agriculture (BUA), Beijing, People's Republic of China
[2] Institute of Microbiology Chinese Academy of Sciences, NO.1 Beichen West Road, Beijing, People's Republic of China
[3] To whom correspondence should be addressed at College of Animal Science and Technology, Beijing University of Agriculture (BUA), Beijing, People's Republic of China. E-mail: liufenghua1209@126.com

of abdominal pain, diarrhea, dysentery, and other diseases in Thailand [10, 11]. α-Mangostin, a major metabolite of mangosteen husks, has notable anti-inflammatory [12, 13], antibacterial [14, 15], and anti-tumor [10, 16] properties. α-Mangostin has been reported to block activation of the LPS-induced in RAW 264.7 cells, thus inhibiting the secretion of NO, COX-2, IL-1β, and IL-6 [17]. However, it has not been reported that α-mangostin would alleviate the LPS inflammatory challenge in IEC-6 cells by inhibiting the TAK1–NF-κB signaling pathway, and this has not yet been reported.

In this study, we established an IEC-6 cell inflammation model using LPS-stimulated cells and determined the effect of α-mangostin on inflammation-related indicators. We also explored changes in the TAK1–NF-κB signaling pathway to study its anti-inflammatory mechanisms and it may be a potential choice for the treatment of inflammation diseases.

MATERIALS AND METHODS

Assessment of Cell Viability by the CCK-8 Assay

IEC-6 cells were purchased from the Cell Resource Center (CRL21592, Beijing, China). Cells were cultured in Dulbecco's modified Eagle medium (DMEM) medium supplemented with 10% fetal bovine serum FBS (Gibco, Grand Island, USA). IEC-6 cells were preincubated overnight in 96-well plates at a density of 1×10^5 cells per well. After 24 h, cells were stimulated with different concentrations of *Escherichia coli* 055:B5 LPS (Sigma-Aldrich Chemical, St. Louis, USA) (0, 1, 5, 10, 20, 40, and 80 μg/ml) for another 24 h. Then, 10 μl CCK-8 (Dojindo, Japan) was added to each well and incubated for 2 h in the dark according to the CCK-8 instruction manual. Optical density was measured at 450 nm using a microplate reader (TECAN, Männedorf, Switzerland). α-Mangostin [> 98% purity by high-performance liquid chromatography] (Tongtian, Shanghai, China) was used at different concentrations (0, 1.25, 2.5, 5, 10, 20, and 40 μM) to stimulate cells for 24 h, then the CCK-8 assay was repeated.

Detection of Apoptosis by Flow Cytometry

IEC-6 cells were preincubated overnight in flasks at a density of 1×10^5 cells/mL. After 24 h, cells were pretreated with α-mangostin (2.5, 5, and 10 μM) for 1 h prior to stimulation with 10 μg/ml LPS for 24 h. Then, cells were harvested and resuspended at 1×10^6 cell/mL, then 5 μl annexin V-FITC and propidium iodide (Becton Dickinson and Company, Lake Franklin, USA) was added. Apoptosis was detected by flow cytometry (Becton Dickinson and Company, Lake Franklin, USA).

Nitric Oxide Assay

Cellular secretion of NO into the supernatant was measured using a total NO detection kit (Beyotime, Haimen, China) by the classic Griess assay detection of nitrite. Briefly, IEC-6 cells were preincubated overnight in flasks at a density of 1×10^5 cells/mL. After 24 h, cells were pretreated with α-mangostin (2.5, 5, and 10 μM) for 1 h prior to stimulation with 10 μg/ml LPS for 24 h. Culture supernatants were mixed with Griess reagent I and Griess reagent II, then incubated at room temperature for 10 min in the dark. Absorbance values were detected at 540 nm, and the NO concentration was calculated using sodium nitrite standard curves.

ELISA Assay

IEC-6 cells were preincubated overnight in flasks at a density of 1×10^5 cells/mL. After 24 h, cells were pretreated with α-mangostin (2.5, 5, and 10 μM) for 1 h prior to stimulation with 10 μg/ml LPS for 24 h. Cellular supernatants were then collected and assayed immediately. PGE2, IL-1β, IL-6, and TNF-α concentrations were measured using ELISA kits (Beyotime, Haimen, China) according to the manufacturer's instructions. Absorbance values were detected at 450 nm.

Q-PCR Analysis

IEC-6 cells were preincubated overnight in flasks at a density of 1×10^5 cells/mL. After 24 h, cells were pretreated with α-mangostin (2.5, 5, and 10 μM) for 1 h prior to stimulation with 10 μg/ml LPS for 24 h. Total RNA was extracted using the Total RNA Kit I (OMEGA, BioTek, USA), and the RNA concentration and integrity were determined using a micro-UV spectrophotometer (JENWAY, UK) at A260/280. Q-PCR analysis was carried out as described previously using the DNA Engine Mx3000P® fluorescence detection system including the SYBR Green PCR mix (Agilent, CA, USA) with a double-stranded DNA-specific fluorescent dye (Stratagene, CA, USA) according to optimized PCR protocols. β-actin was used as a normalization control. The cycling conditions were as follows: 95 °C for 3 min, followed by 40 cycles of 95 °C for 15 s, 60 °C for 30 s, and 72 °C for 60 s. For the Q-PCR reaction system, see Stratagene instructions. The gene-specific oligonucleotide primers used for Q-PCR are listed in Table 1.

Table 1. Gene-Specific Oligonucleotide Primers Used for Q-PCR

Gene	Serial number	Primer sequence	Size of the products (bp)
β-actin	XM_021163894.1	Forward 5′-CCACCATGTACCCAGGCATT-3′ Reverse 5′-AGGGTGTAAAACGCAGCTCA-3′	253
iNOS	XM_006532446.3	Forward 5′-TCTTTGACGCTCGGAACTGTAGCA-3′ Reverse 5′-CGTGAAGCCATGACCTTTCGCATT-3′	976
COX-2	XM_021159633.1	Forward 5′-TTGCTGTACAAGCAGTGGCAAAGG-3′ Reverse 5′-AGGACAAACACCGGAGGGAATCTT-3′	692
IL-6	XM_021163844.1	Forward 5′-GTTCTCTGGGAAATCGTGGA-3′ Reverse 5′-GCATTGGAAATTGGGCTAGG-3′	344
TNF-α	XM_021149738.1	Forward 5′-AAGGGAGAGTGGTCAGGTTGC-3′ Reverse 5′-CAGAGGTTCAGTGATGTAGCG-3′	418
1 L-1β	XM_006498795.3	Forward 5′-GCAGGCAGTATCACTCATTGT-3′ Reverse 5′-GGCTTTTTTGTTGTTCATCTC-3′	221
TLR4	XM_021161091.1	Forward 5′-GCCGGAAAGTTATTGTGGTGG-3′ Reverse 5′-ATGGGTTTTAGGCGCAGAGTT-3′	356
MyD88	XM_021171309.1	Forward 5′-CAACCAGCAGAAACAGGAGTC-3′ Reverse 5′-ATTGGGGCAGTAGCAGATGAA-3′	157

Primers were designed from the published sequences in the GenBank database under the indicated accession numbers. *F* forward primer, *R* reverse primer

Western Blotting Analysis

IEC-6 cells were incubated overnight in culture flasks at a density of 1×10^5 cells/mL. After 24 h, cells were pretreated with α-mangostin (2.5, 5, and 10 μM) for 1 h prior to stimulation with 10 μg/ml LPS for 30 min. Proteins from IEC-6 cells were extracted using a total protein extraction kit (Biochain, Winooski, USA) and quantified using a BCA protein assay kit (Pierce, Rockford, USA) as previously described. Proteins were separated by SDS-PAGE and electro-transferred onto nitrocellulose membranes (Pierce, Rockford, USA), then hybridized with specific antibodies against pIκκ, IκB, pIκB, p65, pp65, TAK1, and pTAK1 (Cell Signaling Technology, Danvers, USA). Blots were normalized using β-actin to correct for differences in loading. Densitometric values of immunoblot signals were obtained from three separate experiments using Image J software (National Institutes of Health, USA).

Immunofluorescence Analysis

IEC-6 cells were tiled on coverslips at a density of 1×10^5 cells/mL overnight in a six-well plate. After 24 h, cells were pretreated with α-mangostin (10 μM) for 1 h prior to stimulation with 10 μg/ml LPS for 30 min. Cells were then fixed with 4% paraformaldehyde for 20 min, blocked with 5% BSA (Beyotime) for 1 h, then hybridized with specific antibodies against p65 (Cell Signaling Technology) at 4 °C. They were then incubated in the dark for 2 h with anti-mouse IgG secondary antibody Alexa Fluor 488 conjugate (Cell Signaling Technology), then stained with DAPI (Cell Signaling Technology) in the dark for 5 min. Cells were finally observed with a laser confocal microscope (Carl Zeiss AG, Oberkochen, Germany).

Statistical Analysis

Data were assessed by one-way analysis of variance using SPSS software. Results are expressed as means ± S.E.M, samples with different superscript letters represent statistically significant differences ($P < 0.05$).

RESULTS

Establishment of an IEC-6 Cell Inflammation Model

To examine the cytotoxicity of various concentrations (0–80 μg/ml) of LPS on IEC-6 cells, cell viability was determined using the CCK-8 assay. LPS 10 μg/ml was shown to have a significant inhibitory effect on cell growth ($P < 0.05$), and cell viability continued to decline as the LPS concentration increased (Fig. 1(a)).

Effect of α-Mangostin on Cell Viability *In Vitro*

To examine the cytotoxicity of various amounts (0–40 μM) of α-mangostin on IEC-6 cells, cell viability was determined using the CCK-8 assay. No cytotoxicity was observed for α-mangostin concentrations ranging from 0 to

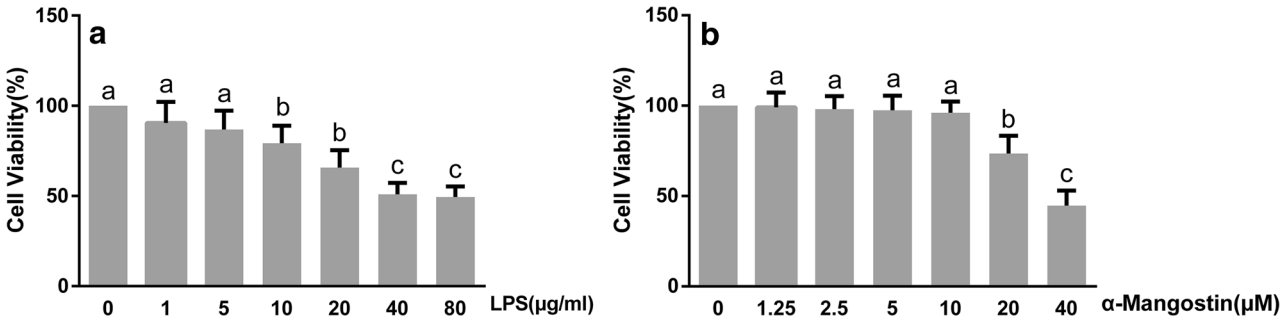

Fig. 1. The effect of LPS and α-mangostin on the viability of IEC-6 cells as measured using a CCK-8 assay. (**a**) LPS cytotoxicity in IEC-6 cells. Cells were incubated with LPS (0–80 μg/ml) for 24 h. (**b**) α-mangostin cytotoxicity in IEC-6 cells. Cells were incubated with α-mangostin (0–40 μM) for 24 h. Data represent the mean ± S.E.M of three independent experiments; samples with different superscript letters represent statistically significant differences ($P < 0.05$).

10 μM, and the concentrations of more than 10 μM has significant damage to cells ($P < 0.05$) (Fig. 1(b)).

α-Mangostin Prevents Apoptosis Induced by LPS

To determine the effect of α-mangostin on LPS-induced apoptosis in IEC-6 cells, we used flow cytometry. The LPS challenge significantly increased apoptosis in IEC-6 cells compared with the control group (Fig. 2(b)) ($P < 0.05$), while pretreatment with α-mangostin (2.5, 5, and 10 μM) significantly decreased apoptosis in a concentration-dependent manner ($P < 0.05$) (Fig. 2(c–e)).

α-Mangostin Prevents Changes in Cell Morphology Induced by LPS

In terms of cell morphology, the LPS challenge resulted in irregular arrangements, shrinkage, the disappearance of

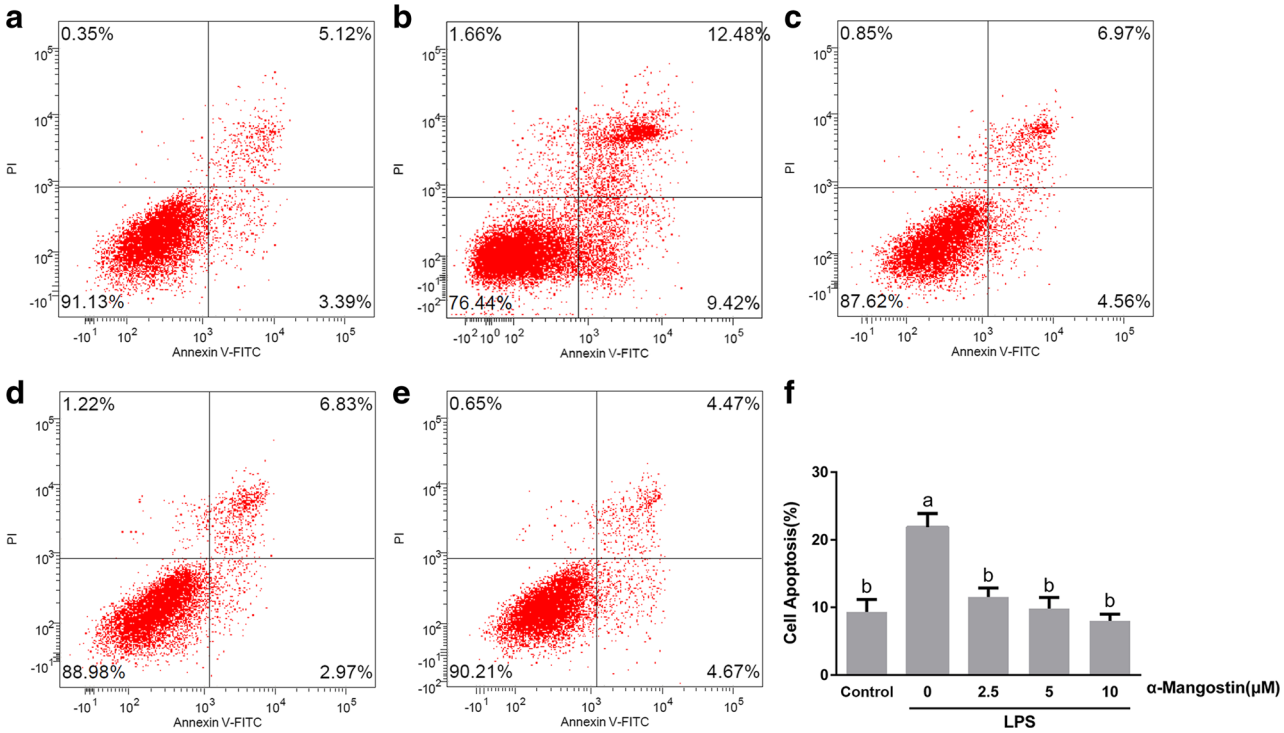

Fig. 2. Effect of α-mangostin on LPS-incubated apoptosis in IEC-6 cells. (**a**) Control cells. (**b**) Cells were incubated with 10 μg/ml LPS for 24 h. (**c**-**e**) Cells were pretreated with α-mangostin (2.5, 5, and 10 μM) for 1 h and exposed to 10 μg/ml LPS for 24 h. (**f**) The number of apoptotic cells under different conditions. Data represent the mean ± S.E.M of three independent experiments; samples with different superscript letters represent statistically significant differences ($P < 0.05$).

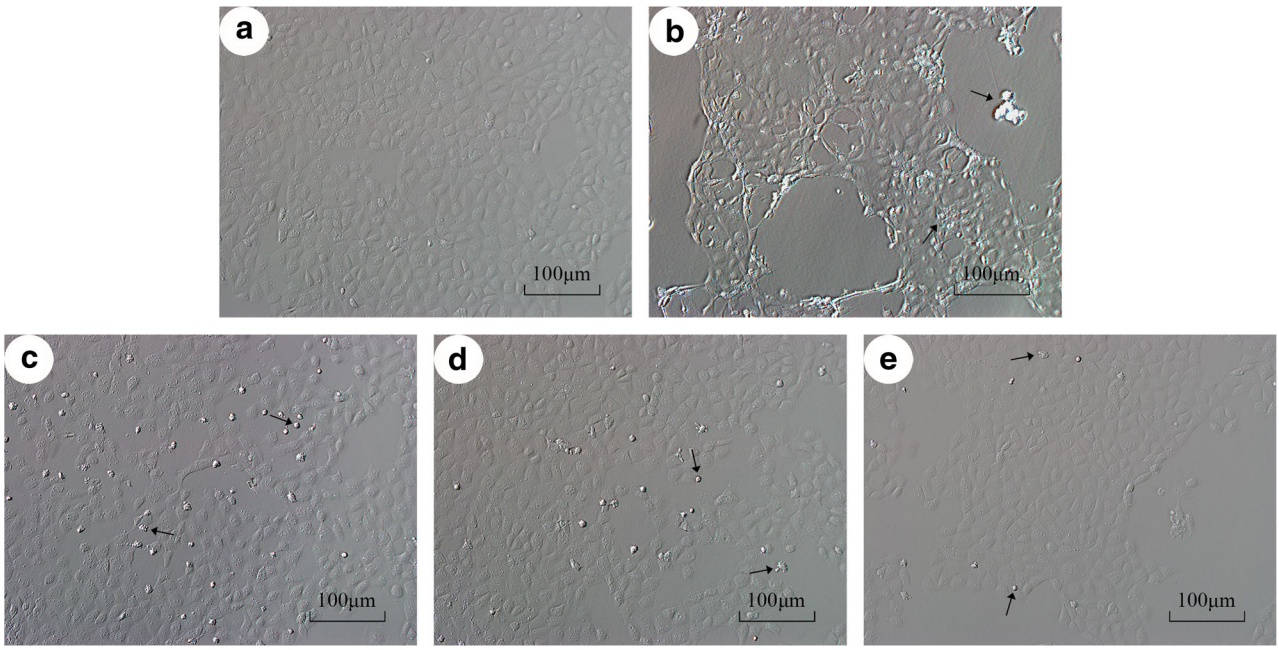

Fig. 3. Effect of α-mangostin on LPS-incubated morphological changes in IEC-6 cells. (**a**) Control cells. (**b**) Cells were incubated with 10 μg/ml LPS for 24 h. (**c**-**e**) Cells were pretreated with α-mangostin (2.5, 5, and 10 μM) for 1 h and exposed to 10 μg/ml LPS for 24 h.

intercellular connections, and massive floating death in IEC-6 cells compared with the control group (Fig. 3(b)), while pretreatment with α-mangostin (2.5, 5, and 10 μM) significantly decreased these changes in a concentration-dependent manner (Fig. 3(c–e)).

α-Mangostin Inhibited the Cytokines and mRNA Expression of LPS-Induced Cytokines

LPS stimulation significantly increased the production of NO, PGE2, IL-6, TNF-α, and IL-1β in IEC-6 cells compared with the control group ($P < 0.05$), while pretreatment with α-mangostin (2.5, 5, and 10 μM) significantly decreased the production of these cytokines in a concentration-dependent manner ($P < 0.05$) (Fig. 4(a–e)).

The LPS challenge also significantly increased iNOS, COX-2, IL-6, TNF-α, and IL-1β expression at the mRNA level in IEC-6 cells ($P < 0.05$); however, α-mangostin (2.5, 5, and 10 μM) pretreatment attenuated this in a concentration-dependent manner ($P < 0.05$) (Fig. 4(f–j)).

α-Mangostin Inhibited the LPS-Induced mRNA Expression of TLR4 and MyD88

We next examined TLR4 and MyD88 mRNA expression levels in IEC-6 cells. LPS stimulation significantly increased TLR4 and MyD88 mRNA expression ($P < 0.05$), while pretreatment with α-mangostin (2.5, 5, and 10 μM) significantly decreased it in a concentration-dependent manner ($P < 0.05$) (Fig. 5).

α-Mangostin Inhibited the TAK1/NF-κB Signaling Pathway

To investigate the anti-inflammatory mechanism of α-mangostin, we examined changes in TAK1–NF-κB signaling pathway-related proteins. Following the LPS challenge of IEC-6 cells, the expression of NF-κB upstream proteins pTAK1 and pIκκ was significantly increased ($P < 0.05$); however, no change was in the expression of TAK1, while pretreatment with α-mangostin (2.5, 5, and 10 μM) significantly decreased pTAK1 and pIκκ expression in a concentration-dependent manner ($P < 0.05$) (Fig. 6).

LPS stimulation of IEC-6 cells induced a significant decrease in IκB expression and increase in pIκB and pp65 expression ($P < 0.05$); however, no change was in the expression of p65, while pretreatment with α-mangostin (2.5, 5, and 10 μM) significantly increased IκB expression and decreased pIκB and pp65 expression in a concentration-dependent manner ($P < 0.05$) (Fig. 7).

Effect of α-Mangostin on the Nuclear Import of p65

We used immunofluorescence to detect the nuclear import of NF-κB subunit p65. In LPS-stimulated IEC-6 cells, p65

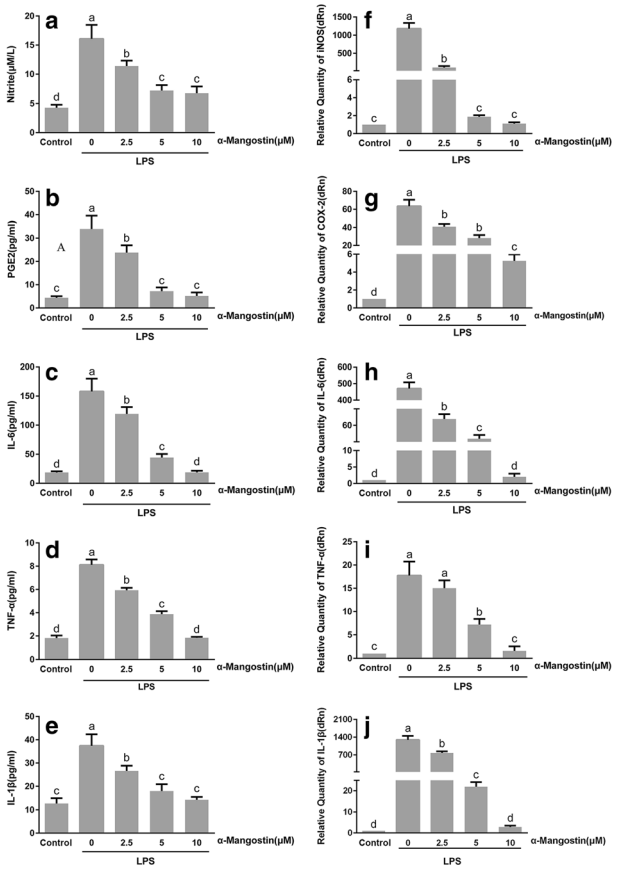

Fig. 4. Effect of α-mangostin on LPS-induced in cytokine expression in IEC-6 cells. (**a**-**e**) Effect of different concentrations of α-mangostin on LPS-induced NO, PGE2, IL-6, TNF-α, and IL-1β expression in IEC-6 cells. NO production in the supernatant was measured using the Griess reaction, while PGE2, IL-6, TNF-α, and IL-1β expression was detected using ELISA. (**f**-**j**) Effect of different concentrations of α-mangostin on LPS-induced iNOS, COX2, IL-6, TNF-α, and IL-1β mRNA expression in IEC-6 cells, as detected by Q-PCR. Cells were pretreated with α-mangostin (2.5, 5, and 10 μM) for 1 h and exposed to 10 μg/ml LPS for 24 h. Data represent the mean ± S.E.M of three independent experiments; samples with different superscript letters represent statistically significant differences ($P < 0.05$).

nuclear import was significantly increased, while pretreatment with α-mangostin (10 μM) significantly decreased p65 nuclear import (Fig. 8).

DISCUSSION

In recent years, studies have found that intestinal mucosal immune dysfunction is closely related to inflammatory bowel disease, ulcerative colitis, and other diseases, while small intestinal mucosal epithelial cells are involved in intestinal digestion, absorption, secretion, and other functions [18]. Therefore, it is of great clinical significance to study the biological characteristics of intestinal epithelial cells directly from *in vitro*. LPS is one of the main components of the cell wall of Gram-negative bacteria and an important factor in inducing inflammation [19]. The study found that LPS-stimulated IEC-6 cells secrete NO, IL-6, and TNF-α [20, 21]. In the present study, we found that different doses of LPS caused IEC-6 injury, while the application of 10 μg/ml LPS for 24 h significantly reduced the viability of IEC-6 cells. Therefore, we used 10 μg/ml LPS to construct an inflammation model and verified that this concentration of LPS caused damage through analysis of cell morphology and flow cytometry.

NO is mainly regulated by iNOS and plays an important role in the immune system [22]. Studies have found that excessive NO activates the NF-κB signaling pathway, thereby promoting movement of the p65 nuclear subunit of NF-κB into the nucleus and inducing the production of pro-inflammatory cells [23]. IL-6, TNF-α, and IL-1β, a key factor in detecting inflammation, can activate iNOS, further promoting NO production and increasing inflammation [24, 25]. PGE2 is mainly regulated by COX-2 as a pro-inflammatory mediator, and PGE2 overexpression can cause the development of many inflammatory diseases [26, 27]. Therefore, we selected NO, PGE2, IL-6, TNF-α, and IL-1β as indicators for evaluating inflammation in the present study. In the present study, we found that LPS causes increased expression of NO, PGE2, IL-6, TNF-α, and IL-1β and is achieved through modulation of iNOS, COX-2, IL-6, TNF-α, and IL-1β mRNA expression.

As a traditional Chinese medicine in Southeast Asia, mangosteen peel has been used to treat abdominal pain, diarrhea, dysentery, and wound infections [28]. Previous studies showed that the co-culture of α-mangostin (0–10 μM) with human periodontal ligament fibroblasts for 24 h had no significant effect on cell viability [29]. Similarly, we found that cell viability was not significantly changed by co-culture of α-mangostin (0–10 μM) with IEC-6 cells for 24 h. Therefore, we used 2.5, 5, and 10 μM to investigate whether α-mangostin could alleviate LPS-induced inflammatory responses in IEC-6 cells. The anti-inflammatory mechanism of α-mangostin is well documented. In independent studies, α-mangostin reduced the LPS-induced secretion of COX-2, IL-6, and IL-1β by RAW 264.7 macrophages [17]. However, the inhibitory effects of α-mangostin on LPS-induced IEC-6 cell inflammation and its mechanisms have not been reported. In the present study, α-mangostin significantly inhibited changes

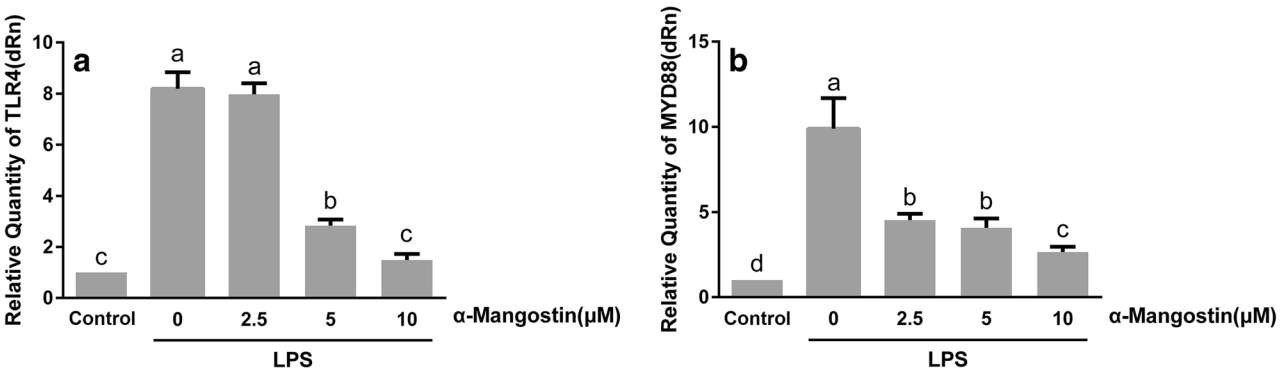

Fig. 5. Effect of α-mangostin on LPS-induced TLR4 and MyD88 mRNA expression. (**a**) Effect of different concentrations of α-mangostin on LPS-induced TLR4 mRNA expression in IEC-6 cells. (**b**) Effect of different concentrations of α-mangostin on LPS-induced MyD88 mRNA expression in IEC-6 cells. Cells were pretreated with α-mangostin (2.5, 5, and 10 μM) for 1 h and exposed to 10 μg/ml LPS for 24 h, mRNA expression detected by Q-PCR; data represent the mean ± S.E.M of three independent experiments; samples with different superscript letters represent statistically significant differences ($P < 0.05$).

to cell morphology induced by LPS and reduced apoptosis. α-Mangostin also significantly reduced LPS-induced increases of NO, PGE2, IL-6, TNF-α, and IL-1β secretion, with 10 μM of α-mangostin having the greatest effect on blocking the transcription of inflammatory cytokines. At the same time, we have found that α-mangostin reduces the expression of inflammatory cytokines by reducing the expression of iNOS, COX-2, IL-6, TNF-α, and IL-1β mRNA.

TLR4 is one of the receptors related to innate immunity and several inflammatory reactions; studies have shown that LPS binds to cell surface TLR4 receptors to recruit MyD88 and activate downstream signaling pathways [30, 31]. Xu et al. also reported that TLR4 mRNA expression was significantly increased after LPS stimulation of RAW 264.7 macrophages [25]. We found that α-mangostin significantly down-regulated the LPS-induced increase in TLR4 and MyD88 mRNA expression, with

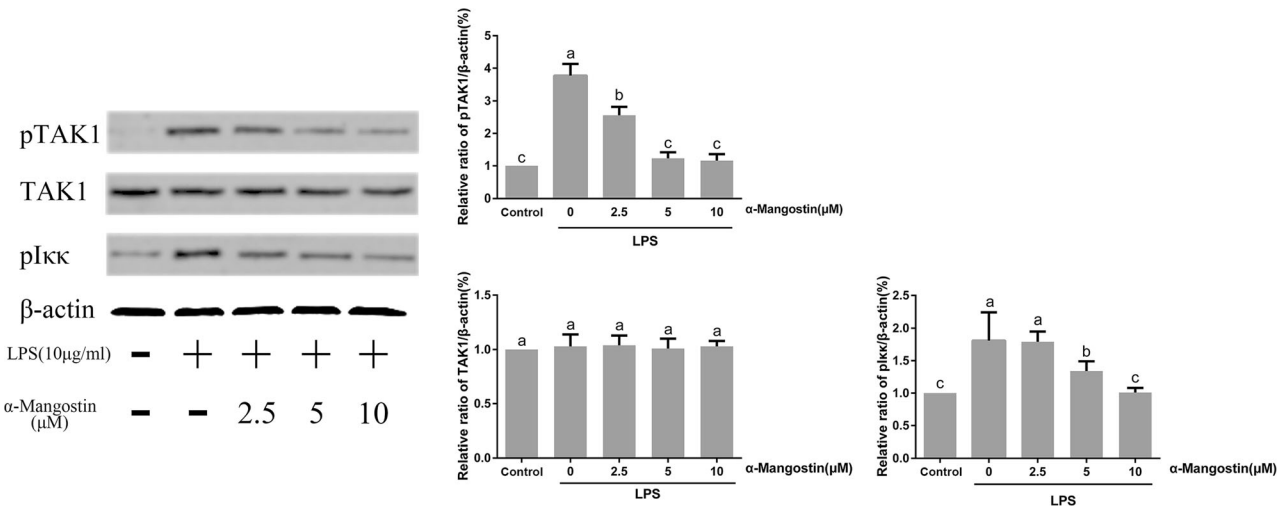

Fig. 6. Effect of α-mangostin on LPS-induced upstream proteins NF-κB signaling pathway in IEC-6 cells. Cells were pretreated with α-mangostin (2.5, 5, and 10 μM) for 1 h and exposed to 10 μg/ml LPS for 30 min; protein (TAK1, pTAK1, pIκκ) expression was analyzed by western blot. Data represent the mean ± S.E.M of three independent experiments; samples with different superscript letters represent statistically significant differences ($P < 0.05$).

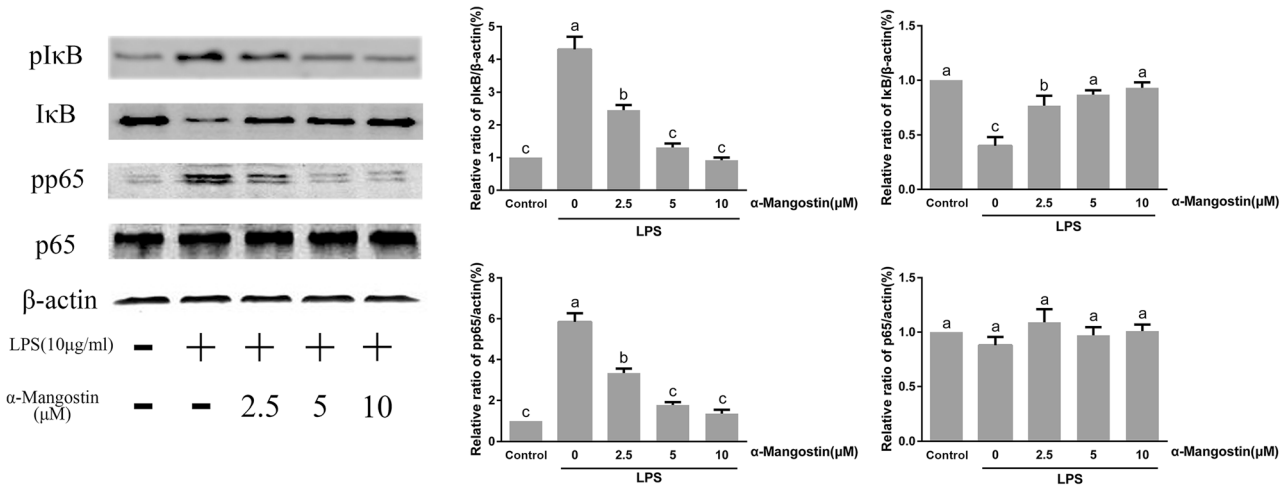

Fig. 7. Effect of α-mangostin on LPS-induced NF-κB signaling pathway activation in IEC-6 cells. Cells were pretreated with α-mangostin (2.5, 5, and 10 μM) for 1 h and exposed to 10 μg/ml LPS for 30 min; protein (IκB, pIκB, p65, pp65) expression was analyzed by western blot. Data represent the mean ± S.E.M of three independent experiments; samples with different superscript letters represent statistically significant differences ($P < 0.05$).

10 μM of α-mangostin being the most effective. This indicates that LPS functions by binding TLR4 receptors and activating MyD88.

NF-κB is an important transcription factor that regulates inflammation [32]. It is typically a heterodimer consisting of five subunits. At rest, NF-κB binds to its inhibitory protein, IκB, in an inactive form in the cytoplasm [33, 34]. Cellular stimulation by inflammatory mediators or LPS relieves the inhibitory effect of IκB on NF-κB, leading to IκB dissociation from the complex and rapid degradation by proteases. After binding to the corresponding site of specific DNA, NF-κB induces gene transcription and promotes the release of cytokines, thereby causing systemic inflammation [35]. TAK1 is a member of the mitogen-activated protein kinase kinase family. It is an upstream regulator of the NF-κB signaling pathway; therefore, inhibiting TAK1/NF-κB activation is an important function of anti-inflammatory drugs [36]. TAK1 indirectly activates the IκB kinase Iκκ which activates NF-κB to participate in pathophysiological processes [37]. Yang et al. found that LPS-stimulated cells exert anti-inflammatory effects by inhibiting TAK1 activation, thus preventing NF-κB activation [38]. In this study, α-mangostin significantly inhibited LPS-induced phosphorylation of NF-κB subunits IκB and p65 and their upstream proteins TAK1 and Iκκ, and significantly inhibited the degradation of NF-κB inhibitor IκB; however, it had no effect on p65 or TAK1. In immunofluorescence experiments, we found that α-mangostin inhibits LPS-induced nucleation of p65. This indicated that α-mangostin inhibits LPS-induced inflammation in IEC-6 cells through TLR4–MyD88–TAK1–NF-κB.

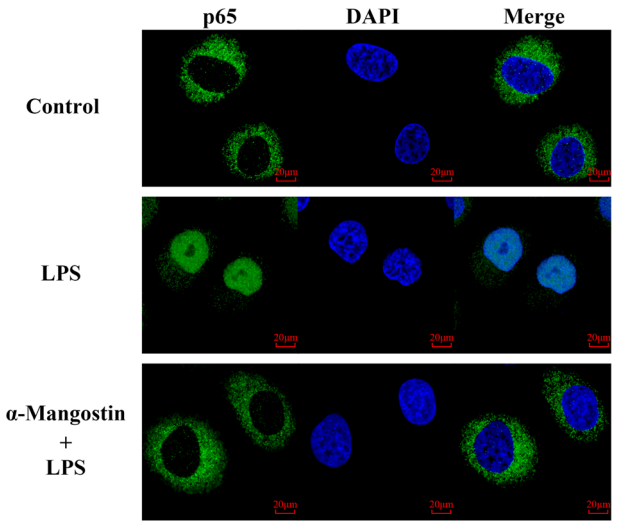

Fig. 8. Effect of α-mangostin on the LPS-induced movement of NF-κB subunit p65 into the nucleus of IEC-6 cells. Cells were pretreated with α-mangostin (10 μM) for 1 h and exposed to 10 μg/ml LPS for 30 min, then stained for p65 (green) and DAPI (blue).

In summary, our investigation revealed that α-mangostin inhibits the LPS-induced release of pro-inflammatory factors and cytokines including NO, PGE2, IL-1β, IL-6, and TNF-α in IEC-6 cells by suppressing the activation of TLR4-mediated TAK1–NF-κB signaling pathways.

FUNDING

This work was supported by grants from the Beijing Municipal Science and Technology Project (D171100002117002).

COMPLIANCE WITH ETHICAL STANDARDS

Conflict of Interest. The authors declare that they have no conflicts of interest.

REFERENCES

1. Glover, Louise E., J. Scott Lee, and Sean P. Colgan. 2016. Oxygen metabolism and barrier regulation in the intestinal mucosa. *Journal of Clinical Investigation* 126 (10): 3680–3688.
2. You, B.H., H.S. Chae, J. Song, H.W. Ko, Y.W. Chin, and Y.H. Choi. 2017. α-Mangostin ameliorates dextran sulfate sodium-induced colitis through inhibition of NF-κB and MAPK pathways. *International Immunopharmacology* 49: 212–221.
3. Nathan, C. 2002. Points of control in inflammation. *Nature* 420 (6917): 846–852. https://doi.org/10.1038/nature01320.
4. Luo, Fen, Rui Zhou, Hui Lei, Yi Mou, Ping Zhang, Yi Sun, Tong Chen, Ling He, and Tianhua Yan. 2016. Umbelliferone attenuates lipopolysaccharide-induced acute lung injury linked with regulation of TLRs–MyD88 and RIP140/NF-κB signaling pathways. *RSC Advances* 6 (100): 97503–97511.
5. Qu, Minye, Tao Xiang, and Jian Ma. 2017. Yi-Qi-Ping-Chuan-Fang reduces TSLP elevation caused by LPS + poly (I:C) via inhibiting TLR4/MYD88/NF-κB signaling pathway. *Evidence-based Complementary and Alternative Medicine* 2017 (3): 3209407.
6. Pham, Tuan-Anh, Changwoo Han, and Haeil Park. 2017. Synthesis of ochnaflavone analogs and their inhibitory activity on PGE2 and NO production against LPS-treated RAW 264.7 cells. *Bulletin of the Korean Chemical Society* 38 (6): 681–683.
7. So, Y., S.Y. Lee, A.R. Han, J.B. Kim, H.G. Jeong, and C.H. Jin. 2016. Rosmarinic acid methyl ester inhibits LPS-induced NO production via suppression of MyD88-dependent and -independent pathways and induction of HO-1 in RAW 264.7 cells. *Molecules* 21 (8): 1083.
8. Mukti, Nur Indah Fajar, Imam Prasetyo, Aswati Mindaryani, and Shofwatunnida' Septarini. 2018. Preparation of porous carbon as ethylene adsorbent by pyrolysis of extraction waste mangosteen rinds.
9. Suttirak, W., and S. Manurakchinakorn. 2014. *In vitro* antioxidant properties of mangosteen peel extract. *Journal of Food Science and Technology* 51 (12): 3546–3558.
10. Ming, Guo, Xiaomeng Wang, Xiaowang Lu, Hongzheng Wang, and Peter E. Brodelius. 2016. α-mangostin extraction from the native mangosteen (Garcinia mangostana L.) and the binding mechanisms of α-mangostin to HSA or TRF. *PLoS One* 11 (9): e0161566.
11. Rukthong, P., N. Sereesongsang, T. Kulsirirat, B. Nimprayoon, and K. Sathirakul. 2017. Effect of α-mangostin on enhanced transdermal bioavailability of gartanin via efflux transporters. *Journal of Bioequivalence and Bioavailability* 09 (4).
12. Nava, Catorce M., G. Acero, J. Pedraza-Chaverri, G. Fragoso, T. Govezensky, and G. Gevorkian. 2016. Alpha-mangostin attenuates brain inflammation induced by peripheral lipopolysaccharide administration in C57BL/6J mice. *Journal of Neuroimmunology* 297: 20–27.
13. Won, Y.S., J.H. Lee, S.J. Kwon, J.Y. Kim, K.H. Park, M.K. Lee, and K.I. Seo. 2014. α-Mangostin-induced apoptosis is mediated by estrogen receptor α in human breast cancer cells. *Food & Chemical Toxicology: An International Journal Published for the British Industrial Biological Research Association* 66: 158–165.
14. Guzmán-Beltrán, Silvia, Miguel Ángel Rubio-Badillo, Esmeralda Juárez, Fernando Hernández-Sánchez, and Martha Torres. 2015. Nordihydroguaiaretic acid (NDGA) and α-mangostin inhibit the growth of Mycobacterium tuberculosis by inducing autophagy. *International Immunopharmacology* 31: 149.
15. Phuong, Nguyen Thi Mai, Ngo Van Quang, Ta Thu Mai, Nguyen Vu Anh, Chutima Kuhakarn, Vichai Reutrakul, and Albert Bolhuis. 2017. Antibiofilm activity of α-mangostin against Staphylococcus aureus. *Asian Pacific Journal of Tropical Medicine* 10 (12).
16. Benjakul, R., L. Kongkaneramit, N. Sarisuta, P. Moongkarndi, and C.C. Müller-Goymann. 2015. Cytotoxic effect and mechanism inducing cell death of α-mangostin liposomes in various human carcinoma and normal cells. *Anti-Cancer Drugs* 26 (8): 824–834.
17. Widowati, Wahyu, Lusiana Darsono, Jo Suherman, Nurul Fauziah, Maesaroh Maesaroh, and Pande Putu Erawijantari. 2016. Anti-inflammatory effect of mangosteen (Garcinia mangostana L.) peel extract and its compounds in LPS-induced RAW264.7 cells. *Natural Product Sciences* 22 (3): 147.
18. Mowat, A.M., and J.L. Viney. 1997. The anatomical basis of intestinal immunity. *Immunological Reviews* 156: 145–166.
19. Rosadini, C.V., and J.C. Kagan. 2017. Early innate immune responses to bacterial LPS. *Current Opinion in Immunology* 44: 14–19. https://doi.org/10.1016/j.coi.2016.10.005.
20. Hu, Ling-Na, Xian Ying Fang, Hai Liang Liu, Zhe Gao, Xue-Feng Wu, Yang Sun, Xu-Dong Wu, and Qiang Xu. 2013. Protective effects of 18β-glycyrrhetinic acid on LPS-induced injury in intestinal epithelial cells. *Chinese Journal of Natural Medicines* 11 (1): 24–29.
21. Talavera, M.M., S. Nuthakki, H. Cui, Y. Jin, Y. Liu, and L.D. Nelin. 2017. Immunostimulated arginase II expression in intestinal epithelial cells reduces nitric oxide production and apoptosis. *Frontiers in Cell and Developmental Biology* 5: 15.
22. Habashi, Soraya Abbasi, Farzaneh Sabouni, Ali Moghimi, and Saeed Ansari Majd. 2016. Modulation of lipopolysaccharide stimulated nuclear factor kappa B mediated iNOS/NO production by bromelain in rat primary microglial cells. *Iranian Biomedical Journal* 20 (1): 33–40.
23. Chen, X., S.A. Tang, E. Lee, Y. Qiu, R. Wang, Duan H. Quan, S. Dan, M. Jin, and D. Kong. 2015. IVSE, isolated from Inula japonica, suppresses LPS-induced NO production via NF-κB and MAPK inactivation in RAW264.7 cells. *Life Sciences* 124: 8–15.
24. Lai, J.L., Y.H. Liu, C. Liu, M.P. Qi, R.N. Liu, X.F. Zhu, Q.G. Zhou, Y.Y. Chen, A.Z. Guo, and C.M. Hu. 2017. Indirubin inhibits LPS-induced inflammation via TLR4 abrogation mediated by the NF-kB and MAPK signaling pathways. *Inflammation* 40 (1): 1–12.
25. Xu, X., P. Yin, C. Wan, X. Chong, M. Liu, P. Cheng, J. Chen, F. Liu, and J. Xu. 2014. Punicalagin inhibits inflammation in LPS-induced

RAW264.7 macrophages via the suppression of TLR4-mediated MAPKs and NF-kappaB activation. *Inflammation* 37 (3): 956–965. https://doi.org/10.1007/s10753-014-9816-2.

26. Li, Tingting, Jianyan Hu, Shanshan Du, Yongdong Chen, Shuai Wang, and Qiang Wu. 2014. ERK1/2/COX-2/PGE2 signaling pathway mediates GPR91-dependent VEGF release in streptozotocin-induced diabetes. *Molecular Vision* 20 (7): 1109–1121.
27. Takeuchi, K., Y. Komatsu, Y. Nakamori, and T. Kotani. 2017. A rat model of ischemic enteritis: pathogenic importance of enterobacteria, iNOS/NO, and COX-2/PGE2. *Current Pharmaceutical Design* 23 (999): 1–1.
28. Chae, H.S., Y.M. Kim, J.K. Bae, S. Sorchhann, S. Yim, L. Han, J.H. Paik, Y.H. Choi, and Y.W. Chin. 2016. Mangosteen extract attenuates the metabolic disorders of high-fat-fed mice by activating AMPK. *Journal of Medicinal Food* 19 (2): 148–154.
29. Kwak, Hyun-Ho, In-Ryoung Kim, Hye-Jin Kim, Bong-Soo Park, and Su Bin Yu. 2016. α-Mangostin induces apoptosis and cell cycle arrest in oral squamous cell carcinoma cell. *Evidence-based Complementary and Alternative Medicine* 2016: 5352412.
30. Wang, Yujue, Guang Chen, Xiangdong Yu, Yunchao Li, Zhang Li, Zongze He, Nannan Zhang, Xiuping Yang, Yansheng Zhao, and Li Na. 2016. Salvianolic acid B ameliorates cerebral ischemia/reperfusion injury through inhibiting TLR4/MyD88 signaling pathway. *Inflammation* 39 (4): 1–11.
31. Yao, H., C. Hu, L. Yin, X. Tao, L. Xu, Y. Qi, X. Han, Y. Xu, Y. Zhao, and C. Wang. 2016. Dioscin reduces lipopolysaccharide-induced inflammatory liver injury via regulating TLR4/MyD88 signal pathway. *International Immunopharmacology* 36: 132–141.
32. Ukil, A., S. Maity, and P.K. Das. 2017. Protection from experimental colitis by theaflavin-3,3′-digallate correlates with inhibition of IKK and NF-kappaB activation. *British Journal of Pharmacology* 180 (1): 121–131.
33. Kim, Sung Hak, Ravesanker Ezhilarasan, Emma Phillips, Daniel Gallegoperez, Amanda Sparks, David Taylor, Katherine Ladner, Takuya Furuta, Hemragul Sabit, and Rishi Chhipa. 2016. Serine/threonine kinase MLK4 determines mesenchymal identity in glioma stem cells in an NF-κB-dependent manner. *Cancer Cell* 29 (2): 201–213.
34. Li, Hong Bao, Xiang Li, Chan Juan Huo, Qing Su, Jing Guo, Zu Yi Yuan, Guo Qing Zhu, Xiao Lian Shi, Jin Jun Liu, and Yu Ming Kang. 2016. TLR4/MyD88/NF-κB signaling and PPAR-γ within the paraventricular nucleus are involved in the effects of telmisartan in hypertension. *Toxicology and Applied Pharmacology* 305: 93–102.
35. Nguyen, D.P., J. Li, S.S. Yadav, and A.K. Tewari. 2014. Recent insights into NF-κB signalling pathways and the link between inflammation and prostate cancer. *BJU International* 114 (2): 168–176.
36. He, Aiqin, Rui Ji, Jia Shao, Chenyun He, Ming Jin, and Yunzhao Xu. 2016. TLR4-MyD88-TRAF6-TAK1 complex-mediated NF-κB activation contribute to the anti-inflammatory effect of V8 in LPS-induced human cervical cancer SiHa cells. *Inflammation* 39 (1): 1–10.
37. Weng, Ting, and Cheng Gee Koh. 2017. POPX2 phosphatase regulates apoptosis through the TAK1-IKK-NF-|[kappa]|B pathway. *Cell Death & Disease* 8 (9): e3051.
38. Yang, S., Z. Yu, T. Yuan, L. Wang, X. Wang, H. Yang, L. Sun, Y. Wang, and G. Du. 2016. Therapeutic effect of methyl salicylate 2-O-β-d-lactoside on LPS-induced acute lung injury by inhibiting TAK1/NF-kappaB phosphorylation and NLRP3 expression. *International Immunopharmacology* 40: 219–228.